A "three-in-one" multi-functional probe for Bcl-2/Mcl-1 profiling and visualizing in situ

Zhang, Xiaodong; Wang, Ziqian; Guo, Zongwei; Song, Ting; He, Nianzhe; Zhu, Junjie; Cao, Keke; Zhang, Zhichao

Published in:
ChemBioChem

Link to article, DOI:
10.1002/cbic.202000441

Publication date:
2021

Document Version
Peer reviewed version

ChemBioChem

Combining Chemistry and Biology

Chemistry Europe

European Chemical Societies Publishing

Accepted Article

Title: A “three-in-one” multi-functional probe for Bcl-2/Mcl-1 profiling and visualizing in situ

Authors: Xiaodong Zhang, Ziqian Wang, Zongwei Guo, Ting Song, Nianzhe He, Junjie Zhu, Keke Cao, and Zhichao Zhang

To be cited as: *ChemBioChem* 10.1002/cbic.202000441

Link to VoR: https://doi.org/10.1002/cbic.202000441

WILEY-VCH

10.1002/cbic.202000441

A "three-in-one" multi-functional probe for Bcl-2/Mcl-1 profiling and visualizing *in situ*

Xiaodong Zhang[a], Dr. Ziqian Wang[b]*, Zongwei Guo[c], Dr. Ting Song[a], Nianzhe He[a,d], Junjie Zhu[a], Keke Cao[a], and Prof. Zhichao Zhang[a]*

[a.] State Key Laboratory of Fine Chemicals, School of Chemistry, Dalian University of Technology, Dalian, China.

[b.] Zhang Dayu School of Chemistry, Dalian University of Technology, Dalian, China.

[c.] School of Life Science and Technology, Dalian University of Technology, Dalian, China.

[d.] Department of Chemistry, Technical University of Denmark, Lyngby, Denmark.

* Corresponding author. E-mail: zczhang@dlut.edu.cn;

10.1002/cbic.202000441

Abstract:

A "three-in-one" multifunctional probe was designed by integrating the Bcl-2/Mcl-1 binding ligand, fluorescent reporter group and photoreactive group into the same scaffold, and further applied for protein profiling and bioimaging of both Bcl-2 and Mcl-1 *in situ*.

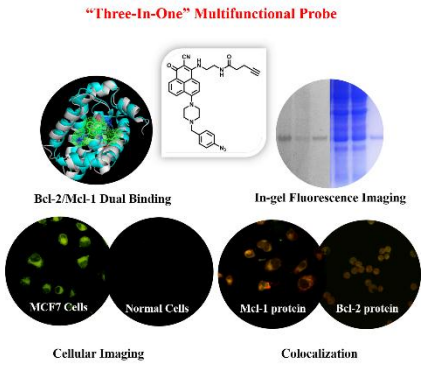

Abstract:

Bcl-2 and Mcl-1, the two arms of the anti-apoptotic Bcl-2 family proteins, have been identified as key regulators of apoptosis and effective therapeutic targets of cancer. However, no small molecular probe is capable of profiling and visualizing both Bcl-2 and Mcl-1 simultaneously *in situ*. Herein, we reported a multi-functional molecular probe (**BnN_3-OPD-Alk**) by a "three-in-one" molecular designing strategy, which integrated the Bcl-2/Mcl-1 binding ligand, fluorescent reporter group and photoreactive group azido into the same scaffold. **BnN_3-OPD-Alk** exhibited sub-μM affinities to Bcl-2/Mcl-1 and bright green self-fluorescence. It was then successfully applied for Bcl-2/Mcl-1 labelling, capturing, enriching, and bioimaging both *in vitro* and in cells. This strategy could facilitate the precise early diagnosis and effective therapy of dual Bcl-2/Mcl-1-related diseases.

Keyword: multi-functional probe; ABPP; Bioimaging; Protein labeling; Bcl-2/Mcl-1 proteins;

10.1002/cbic.202000441

Evasion of apoptosis is one of hallmarks of cancer.[1] As major regulators of mitochondrial apoptosis, B-cell lymphoma 2 (Bcl-2) family proteins are fundamental to the balance between cell death and survival.[2–8] Among them, anti-apoptotic members Bcl-2 and Mcl-1 are frequently upregulated in cancer,[9–14] including breast cancer, prostate cancer, small cell lung cancer, and melanoma, which has been associated with tumor progression and drug resistance.[5,12,15–18] Moreover, Bcl-2 and Mcl-1, known as the two arms of the anti-apoptotic proteins, cooperate to inhibit apoptosis in cancer cells, and therefore effective apoptosis inducers are required to inhibit both functions of them. For example, the increased stability and level of Mcl-1 protein could be observed in ABT-199 (a FDA-approved drug targeting Bcl-2 protein)-resistant cells and thus lead to the failure to apoptosis. Thus, it is the key point to precisely monitor and trace the expression of both Bcl-2 and Mcl-1 proteins in early diagnosis and cancer therapy.

In the past decade, activity-based protein profiling (ABPP) has become a powerful approach for profiling and bioimaging of many therapeutic targets for bioactive molecules *in situ*.[19] Activity-based probes (ABPs) are constituted by three functional modules: a target binding group, a reporter group for target imaging and profiling, and a photoreactive group for covalent probe-target crosslinking. Several probes for Bcl-2 or Mcl-1 imaging has been established by conjugating a fluorophore as reporter tag to ABT-199 or indole-based Bcl-2/Mcl-1 inhibitors.[20–23,24–26] However, the large fluorophore may lead to loss of binding affinity, off-target binding and tedious synthetic route, and noncovalent probe-target complex may not survive the *in vitro* affinity purification process needed for protein profiling. To solve these limitations, Li et al. created a probe by conjugating ABT-199 with an "minimalist linker", in which the photoreactive and reporter groups are made as small as possible, and realized Bcl-2 profiling and bioimaging in both cancer cells and tumor tissues.[27] Nevertheless, the profiling and bioimaging strategy using the ABT-199-derived probe needs an additional procedure to conjugate a fluorophore via "click chemistry" catalyzed by Cu(I), in which metal's cytotoxicity and low reaction efficiency would interfere with the profiling and bioimaging in biological systems.[28,29] Moreover, all covalent probes just focused on detecting Bcl-2 or Mcl-1, respectively, rather than both of them. Therefore, a novel strategy are urgently needed to solve these problems.

Herein, a "three-in-one" multi-functional probe (**BnN_3-OPD-Alk**) was designed by integrating the target binding ligand, reporter group and photoreactive group into the same scaffold, in order to

10.1002/cbic.202000441

realize profiling and bioimaging of both Bcl-2 and Mcl-1 *in situ*. A well-studied Bcl-2/Mcl-1 dual inhibitor **S1**,[30–33] was chosen as the target binding ligand, and then an aryl azide photoreactive group was embedded in a more hydrophobic environment (P2 pocket) for covalent target labeling by replacing the thiomorpholine group with the substituted piperazine group. Finally, 3-cyano group were replaced by an alkyl amino group, which exhibits excellent fluorescence performance in the core scaffold, leading to the "three-in-one" probe **BnN$_3$-OPD-Alk** (Figure 1).

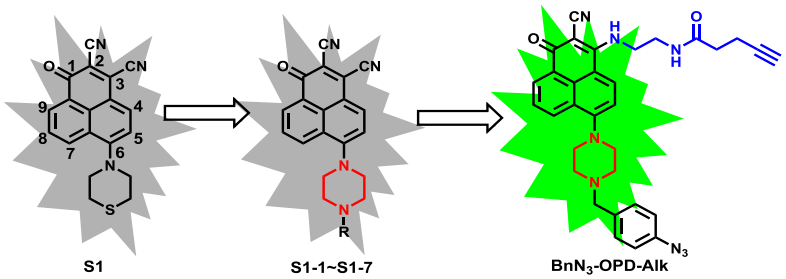

Figure 1. Design of a multi-functional molecular probe for Bcl-2/Mcl-1 proteins.

Published molecular structure characteristics of **S1**/Bcl-2 and **S1**/Mcl-1 complexes have showed that the 6-thiomorpholine group of **S1** located in the deepest hydrophobic P2 pocket of these proteins (Figure S1).[33] Considering more hydrophobic environment will lead to higher labeling efficiency of photoreactive groups,[35] we firstly decided to replace the 6-thiomorpholine by a variety of substituted piperazine groups for better P2 occupation, yielding **S1-1**~**S1-6** (Figure 2A). These compounds were synthesized readily by nucleophilic substitution reaction between 1-oxo-1*H*-phenalene-2,3-dicarbonitrile with corresponding substituted piperazines (Scheme S1),[32] and then binding affinity was tested by fluorescence polarization assay (FPA), using Bcl-2/Mcl-1 dual inhibitor (-)-gossypol as control. As shown in Figure 2B, **S1-4** with benzyl group exhibited the most potent binding capability to both Bcl-2 (*K*i = 0.06 ±0.01 μM) and Mcl-1 (*K*i = 0.07 ±0.02 μM). Molecular docking simulation further illustrated that the benzyl piperazine group of **S1-4** extended into the P2 pocket like the thiomorpholine group of **S1**,[35] which provided a suitable hydrophobic site for photoreactive group embedding (Figure S1). Therefore, an azide moiety for covalent labeling target proteins was installed to the 4-position of benzyl group in **S1-4**. As expected, the resulting compound **S1-7** retained binding potency of **S1-4** (Figure 2B).

Additionally, the 3-cyano was substituted with a primary amine group to obtain a better

10.1002/cbic.202000441

fluorescence performance in the core scaffold due to reduced internal charge transfer (ICT)[36] and terminal alkyne was introduced herein for further target enrichment and identification, yielding the "three-in-one" multi-functional molecular probe **BnN$_3$-OPD-Alk**.

BnN$_3$-OPD-Alk was synthesized using the synthetic route outlined in Scheme S2. FPA showed that **BnN$_3$-OPD-Alk** retained the potent binding capability to both Bcl-2 and Mcl-1 (*K*i =0.08 ± 0.02 μM and 0.10 ± 0.02 μM, Figure S2). Moreover, **BnN$_3$-OPD-Alk** dispalyed a considerable fluorescence quantum yield of 0.056, with the maximum emission wavelength at 566 nm in PBS (pH = 7.4, Table S1). These results rendered the potential of **BnN$_3$-OPD-Alk** for Bcl-2/Mcl-1 labeling, enriching, and imaging studies.

(A)

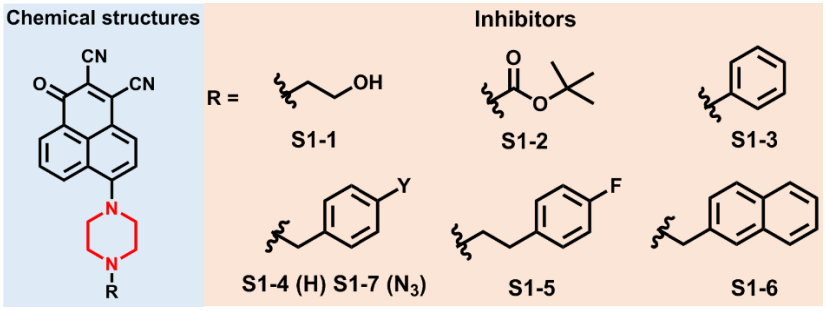

(B)

Ki (μM)	(-)-gossypol	S1-1	S1-2	S1-3	S1-4	S1-5	S1-6	S1-7
Mcl-1	0.20±0.03	0.38±0.02	0.55±0.10	0.39±0.06	0.07±0.02	0.24±0.02	0.15±0.02	0.10±0.03
Bcl-2	0.44±0.06	0.47±0.01	0.72±0.09	0.63±0.09	0.06±0.01	0.83±0.14	0.12±0.03	0.07±0.01

Figure 2. (A) Structures of compounds **S1-1**~**S1-7** and K_i values of **S1-1**~**S1-7** against recombinant Bcl-2/Mcl-1 proteins (B). (-)-gossypol was used as a positive control. The values are the mean ±SD of at least three independent experiments.

To evaluate the labeling efficiency of the probe, the concentration-dependent labeling experiment was first evaluated in mixture of recombinant Bcl-2/Mcl-1 proteins. After incubation of different concentration of **BnN$_3$-OPD-Alk** (2.5/5/10 μM) to the mixture solution of Bcl-2 (5 μM) and Mcl-1 (5 μM) for 2 h, the resulting mixture was exposed to UV light (365 nm) for 20 min. Then, the labeled proteins were separated by SDS-PAGE and visualized by in-gel fluorescence scanning and Coomassie Brilliant Blue (CBB) staining. As shown in Figure 3A, the labeling band by **BnN$_3$-OPD-Alk** can be visible at a probe concentration of 2.5 μM, and showed a concentration-dependent manner till 10 μM, indicating a successful labeling.

10.1002/cbic.202000441

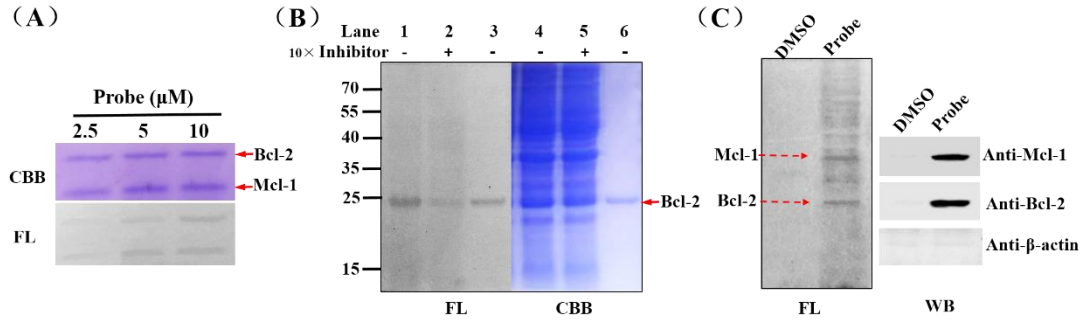

Figure 3. (A) Concentration-dependent labeling of recombinant Bcl-2 and Mcl-1 with **BnN$_3$-OPD-Alk** simultaneously; (B) Labeling profiles of *E.coli* lysates treated with **BnN$_3$-OPD-Alk** in the absence or presence of inhibitor ABT-737 (lanes 1 and 2) and recombinant Bcl-2 treated with **BnN$_3$-OPD-Alk** (lane 3 and 6) (UV irradiation for 20 min); (C) Proteome reactivity profiles of the proteins enriched by **BnN$_3$-OPD-Alk** from MCF-7 cells; the protein was further verified through Western blotting. FL=in-gel fluorescence scanning, CBB=Coomassie gel, WB=Western blotting.

We next determined the selective labeling profiles for Bcl-2 protein in complex environments. Firstly, **BnN$_3$-OPD-Alk** (10 μM) was incubated in the lysate of Escherichia coli BL21 (DE3) (*E.coli*) cells transfected with the plasmid expressing Bcl-2 protein, in the absence or presence of Bcl-2 inhibitor ABT-737 for 2 h, followed by UV irradiation and SDS-PAGE analysis (Figure 3B). A strong fluorescence labeled band was found at ~23 KD, the Mw of recombinant Bcl-2 (lane 1), which diminished when ABT-737 was added (lane 2), and no other obvious fluorescence labeled bands were visible. These results demonstrated the extraordinary potency and selectivity of **BnN$_3$-OPD-Alk** for Bcl-2 fluorescent labeling, and further defined its potential utility as a chemical tool for Bcl-2 family inhibitors screening *in situ*. Therefore, 7 compounds, including commercial Bcl-2 inhibitors (**I1**: ABT-737, **I2**: (-)-gossypol) and candidate molecules (**I3-I7**) (Figure S3), were added as competitors to the system described above. As showed in Figure S4, the fluorescence bands of **BnN$_3$-OPD-Alk** labeled Bcl-2 were significantly decreased in the presence of 10-fold ABT-737 (lane 2), (-)-gossypol (lane 3), and **I5** (lane 6), respectively, illustrating **I5** as a potent Bcl-2 inhibitor. The binding potency of compound **I5** to Bcl-2 was further validated by FPA (K_i = 0.90 ± 0.03 μM), and therefore verified the utility of **BnN$_3$-OPD-Alk** for screening.

Furthermore, capability and selectivity of **BnN$_3$-OPD-Alk** for Bcl-2/Mcl-1 labeling and enrichment *in situ* was tested in human MCF-7 cells. Upon incubation of **BnN$_3$-OPD-Alk** (5 μM)

with live MCF-7 cells for 12 h, the cells were irradiated with UV and lysed; the resulting mixtures were conjugated with biotin-N_3, followed by SDS-PAGE analysis and in-gel fluorescence scanning (Figure 3C). The fluorescently labeled bands at ~26 KD and ~37 KD were further proven to be Bcl-2 and Mcl-1, respectively, by pull-down/western blotting with the corresponding antibodies, highlighting the labeling and enriching capability and specificity of **BnN$_3$-OPD-Alk** *in situ*.

On the basis of the labeling capability of **BnN$_3$-OPD-Alk** toward Bcl-2/Mcl-1, bioimaging experiments were carried out for detecting cellular expression of Bcl-2/Mcl-1. The Bcl-2/Mcl-1-positive cell (MCF-7) was selected as a biological model and the Bcl-2/Mcl-1-negative cell (Dendritic Cells, DC) was used as a negative model. After incubation of **BnN$_3$-OPD-Alk** (5 μM) with cells for 2 h and then imaging, we observed strong green fluorescence in MCF-7 cells and a significant decrease in MCF-7 cells treated with ABT-737, but not in Bcl-2/Mcl-1-negative cells (Figure 4A), supporting the application of **BnN$_3$-OPD-Alk** in detecting endogenous Bcl-2/Mcl-1 proteins.

Furthermore, co-localization experiments demonstrated that the green fluorescence signals of **BnN$_3$-OPD-Alk** was well co-localized with the red signals of corresponding antibodies in Mcl-1-positive cells (H23 cells, Pearson's coefficient is 0.89) (Figure 4B) and Bcl-2-positive cells (HL-60 cells, Pearson's coefficient is 0.85) (Figure 4C), respectively. In addition, in order to verify the location of our probe, the co-localization experiments were performed by co-staining HL-60 cells with probe and Nucleus-Tracker DAPI. As shown in Figure S5, the fluorescence signals of the probe responding to Bcl-2 exhibited almost no overlapping with that of DAPI, indicated that the probe staining mainly located in cytoplasm. These imaging data together suggest that **BnN$_3$-OPD-Alk** is suitable for simultaneous measurement of distribution of Bcl-2/Mcl-1 proteins and imaging in live cells.

10.1002/cbic.202000441

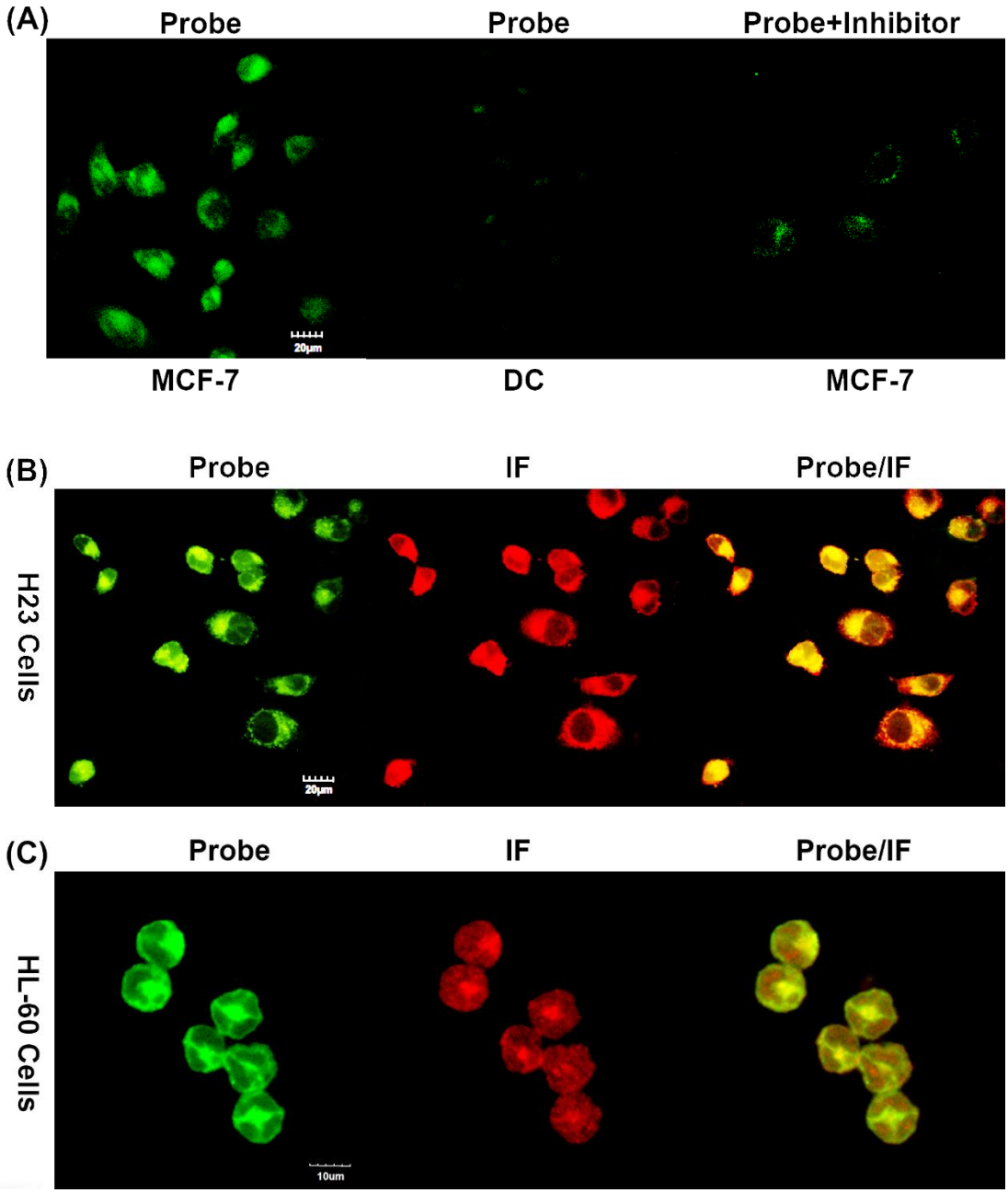

Figure 4 Cellular imaging of **BnN$_3$-OPD-Alk** (5 μM) with MCF-7 and DC cells in the absence or presence of inhibitor ABT737 (A). Co-localization of **BnN$_3$-OPD-Alk** (5 μM) with corresponding antibodies in H23 cells (B) and in HL-60 cells (C). IF=immunofluorescence.

We have developed a multi-functional molecular probe, **BnN$_3$-OPD-Alk**, for Bcl-2/Mcl-1 proteins by the "three-in-one" molecular strategy. The probe exhibited sub-μM binding abilities to both Bcl-2 and Mcl-1, and strong green fluorescence, effective covalent bonding and enriching and was further applied for simultaneous labelling, enriching, and bioimaging of Bcl-2 and Mcl-1 proteins *in situ*. This novel strategy could facilitate the precise early diagnosis and effective therapy of dual Bcl-2/Mcl-1-related diseases.

This research was supported by the National Natural Science Foundation of China (81903462 and 81430083) and the China Postdoctoral Science Foundation (2018M641694).

Conflicts of interest

There are no conflicts to declare.

Notes and references

1 D. Hanahan and R. A. Weinberg, *Cell*, 2011, **144**, 646–674.

2 J. M. Adams and S. Cory, *Trends Biochem. Sci.*, 2001, **26**, 61–66.

3 A. Strasser, L. O. Connor and V. M. Dixit, *Annu. Rev. Biochem.*, 2000, **69**, 217–45.

4 J. Kale, E. J. Osterlund and D. W. Andrews, *Cell Death Differ.*, 2018, **25**, 65–80.

5 A. Burlacu, *J. Cell. Mol. Med.*, 2003, **7**, 249–257.

6 C. Death, D. T. Chao and S. J. Korsmeyer, *Annu Rev Immunol*, 1998, **16**, 395-419.

7 J. M. Adams and S. Cory, *Science*, 1998, **281**, 1322–1326.

8 J. C. Reed, Oncogene, 1998, **17**, 3225–3236.

9 S. K. Tahir, X. Yang, M. G. Anderson, S. E. Morgan-Lappe, A. V. Sarthy, J. Chen, R. B. Warner, S. C. Ng, S. W. Fesik, S. W. Elmore, S. H. Rosenberg and C. Tse, *Cancer Res.*, 2007, **67**, 1176–1183.

10 M. F. van Delft, A. H. Wei, K. D. Mason, C. J. Vandenberg, L. Chen, P. E. Czabotar, S. N. Willis, C. L. Scott, C. L. Day, S. Cory, J. M. Adams, A. W. Roberts and D. C. S. Huang, *Cancer Cell*, 2006, **10**, 389–399.

11 M. Konopleva, R. Contractor, T. Tsao, I. Samudio, P. P. Ruvolo, S. Kitada, X. Deng, D. Zhai, Y. X. Shi, T. Sneed, M. Verhaegen, M. Soengas, V. R. Ruvolo, T. McQueen, W. D. Schober, J. C. Watt, T. Jiffar, X. Ling, F. C. Marini, D. Harris, M. Dietrich, Z. Estrov, J. McCubrey, W. S. May, J. C. Reed and M. Andreeff, *Cancer Cell*, 2006, **10**, 375–388.

12 J. M. Adams and S. Cory, *Oncogene*, 2007, **26**, 1324–1337.

13 T. P. Garner, A. Lopez, D. E. Reyna, A. Z. Spitz and E. Gavathiotis, *Curr. Opin. Chem. Biol.*, 2017, **39**, 133–142.

14 C. M. Pfeffer and A. T. K. Singh, *Int. J. Mol. Sci.*, 2018;19(2):448.

15 W. J. Placzek, J. Wei, S. Kitada, D. Zhai, J. C. Reed and M. Pellecchia, *Cell Death Dis.*, 2010, **1**, 1–9.

16 S. H. Wei, K. Dong, F. Lin, X. Wang, B. Li, J. J. Shen, Q. Zhang, R. Wang and H. Z. Zhang,

Cancer Chemother. Pharmacol., 2008, **62**, 1055–1064.

17 I. E. Wertz, S. Kusam, C. Lam, T. Okamoto, W. Sandoval, D. J. Anderson, E. Helgason, J. A. Ernst, M. Eby, J. Liu, L. D. Belmont, J. S. Kaminker, K. M. O'Rourke, K. Pujara, P. B. Kohli, A. R. Johnson, M. L. Chiu, J. R. Lill, P. K. Jackson, W. J. Fairbrother, S. Seshagiri, M. J. C. Ludlam, K. G. Leong, E. C. Dueber, H. Maecker, D. C. S. Huang and V. M. Dixit, *Nature*, 2011, **471**, 110–114.

18 G. Wei, A. A. Margolin, L. Haery, E. Brown, L. Cucolo, B. Julian, S. Shehata, A. L. Kung, R. Beroukhim and T. R. Golub, *Cancer Cell*, 2012, **21**, 547–562.

19 H. Guo and Z. Li, *Medchemcomm*, 2017, **8**, 1585–1591.

20 M. J. Niphakis and B. F. Cravatt, *Annu. Rev. Biochem.*, 2014, **83**, 341–377.

21 L. E. Sanman and M. Bogyo, *Annu. Rev. Biochem.*, 2014, **83**, 249–273.

22 Z. Li, D. Wang, L. Li, S. Pan, Z. Na, C. Y. J. Tan and S. Q. Yao, *J. Am. Chem. Soc.*, 2014, **136**, 9990–9998.

23 Z. Li, P. Hao, L. Li, C. Y. J. Tan, X. Cheng, G. Y. J. Chen, S. K. Sze, H. M. Shen and S. Q. Yao, *Angew. Chemie - Int. Ed.*, 2013, **52**, 8551–8556.

24 T. Liu, Y. Gao, X. Zhang, Y. Wan, L. Du, H. Fang and M. Li, *Anal. Chem.*, 2017, **89**, 11173–11177.

25 T. Liu, G. Dong, F. Xu, B. Han, H. Fang, Y. Huang, Y. Zhou, L. Du and M. Li, *Anal. Chem.*, 2019, **91**, 5722–5728.

26 R. J. Giedt, M. M. Sprachman, K. S. Yang and R. Weissleder, *Bioconjug. Chem.*, 2014, **25**, 2081–2085.

27 D. Zhu, H. Guo, Y. Chang, Y. Ni, L. Li, Z. M. Zhang, P. Hao, Y. Xu, K. Ding and Z. Li, *Angew. Chemie - Int. Ed.*, 2018, **57**, 9284–9289.

28 J. C. Jewett, E. M. Sletten and C. R. Bertozzi, *J. Am. Chem. Soc.*, 2010, **132**, 3688–3690.

29 J. C. Jewett and C. R. Bertozzi, *Chem. Soc. Rev.*, 2010, **39**, 1272–1279.

30 Z. Zhang, L. Jin, X. Qian, M. Wei, Y. Wang, J. Wang, Y. Yang, Q. Xu, Y. Xu and F. Liu, *ChemBioChem*, 2007, **8**, 113–121.

31 Y. Xiao, F. Liu, Z. Chen, W. Zhu, Y. Xu and X. Qian, *Chem. Commun.*, 2015, **51**, 6480–6488.

32 Z. Zhang, T. Song, T. Zhang, J. Gao, G. Wu, L. An and G. Du, *Int. J. Cancer*, 2011, **128**, 1724–1735.

10.1002/cbic.202000441

33 Z. Zhang, G. Wu, F. Xie, T. Song and X. Chang, *J. Med. Chem.*, 2011, **54**, 1101–1105.

34 T. Song, X. Li, X. Chang, X. Liang, Y. Zhao, G. Wu, S. Xie, P. Su, Z. Wu, Y. Feng and Z. Zhang, *Bioorganic Med. Chem.*, 2013, **21**, 11–20.

35 J. Cheng and T. J. Deming, *Pept. Mater.*, 2011, **310**, 1–26.

36 R. Badugu, J. R. Lakowicz and C. D. Geddes, *J. Am. Chem. Soc.*, 2005, **127**, 3635–3641.